Received: 17 October 2019 | Revised: 15 January 2020 | Accepted: 16 January 2020

DOI: 10.1002/ardp.201900308

DPhG ARCH PHARM
Archiv der Pharmazie

FULL PAPER

Synthesis and biological evaluation of pyrazolone analogues as potential anti-inflammatory agents targeting cyclooxygenases and 5-lipoxygenase

Mohamed A. Shabaan[1] | Aliaa M. Kamal[1,2] | Samar I. Faggal[1] | Ayman E. Elsahar[3] | Khaled O. Mohamed[1]

[1]Department of Pharmaceutical Organic Chemistry, Faculty of Pharmacy, Cairo University, Cairo, Egypt

[2]Department of Pharmaceutical Chemistry, Faculty of Pharmacy, October University for Modern Science and Arts (MSA), Giza, Egypt

[3]Department of Pharmacology and Toxicology, Faculty of Pharmacy, Cairo University, Cairo, Egypt

Correspondence
Khaled O. Mohamed, Department of Pharmaceutical Organic Chemistry, Faculty of Pharmacy, Cairo University, Cairo 11562, Egypt.
Email: khaled.mohamed@pharma.cu.edu.eg

Abstract

New pyrazolone derivatives structurally related to celecoxib and FPL 62064 were synthesized and biologically evaluated for their inhibitory activity against cyclooxygenases (COXs) and 5-lipoxygenase (5-LOX) and their selectivity indices were calculated. The results showed that compounds **3f**, **3h**, **3l**, and **3p** have an excellent COX-2 selectivity index. Moreover, they showed potent 5-LOX inhibitory activity relative to celecoxib and zileuton, as positive controls. These promising candidates were further investigated for anti-inflammatory activity using the carrageenan-induced rat paw edema method and ulcerogenic liability. The results showed no ulceration, which implies their gastric safety profile. Moreover, these compounds were evaluated for prostaglandin (PGE2) production in rat serum. Molecular docking in the COX-2 and 5-LOX active sites was performed to rationalize their anti-inflammatory activities. Strong binding interactions and effective docking scores were identified. The results indicated that these derivatives are good leads for dual-acting COX-2/5-LOX inhibitors to be used as potent and safe anti-inflammatory agents.

KEYWORDS
5-LOX, anti-inflammatory, COX-2 inhibitors, PGE2, pyrazolone

1 | INTRODUCTION

Design of nonsteroidal anti-inflammatory drugs (NSAIDs) with an enhanced safety profile is still a challenge for the pharmaceutical industry. They are used in short-term treatment for common pain, as well as in the long-term management of chronic inflammatory diseases, such as osteoarthritis and rheumatoid arthritis.[1] In spite of the great safety of known NSAIDs over the steroidal derivatives, they still have side effects, including development of peptic and duodenal ulcers, renal failure,[2] liver malfunctions,[3] and strokes.[4] Cyclooxygenase-2 (COX-2) inhibitors were introduced to overcome NSAID-related GI toxicity; however, they increase cardiovascular risk, due to a decrease in endothelial prostaglandin I2 (PGI2) and increased levels of platelet aggregator thromboxane A2 (TXA2).[5] Traditional NSAIDs and coxibs are coupled but with greater risk of cardiovascular problems and stroke.[6] Prostaglandins (PGs) from the cyclooxygenase pathway and leukotrienes (LTs) from the lipoxygenase pathway are both mediators of the inflammatory process generated from the same arachidonic acid (AA) cascade.[7] Severe side effects of coxibs indicate that the biosynthetic pathway may switch the metabolism to other, which has fatal side effects.[8,9] Therefore, compounds that may inhibit COX-2/5-LOX together will consequently shut off the production of mediators of inflammation from the AA pathway; thus, dual inhibition of COX-2/5-LOX enzymes establishes a rational

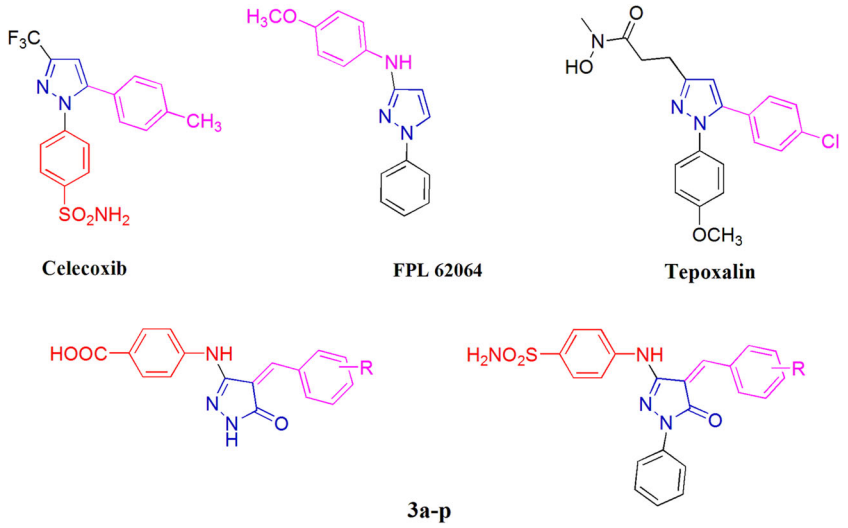

FIGURE 1 Structures of dual COX-2/5-LOX inhibitors containing pyrazole moiety (celecoxib, FBL 62064, and tepoxalin) and design strategy for the target compounds

method for the development of new anti-inflammatory (AI) agents with a good safety profile.[10] Compounds inhibiting both COX-2 and 5-LOX pathways may possess higher AI efficacy accompanied by lower gastric toxicity in comparison with traditional COX inhibitors.[11] Dual COX-2/5-LOX inhibitors containing pyrazole moiety include celecoxib and FPL 62064 (*N*-(4-methoxyphenyl)-1-phenyl-1*H*-pyrazol-3-amine), which is a dual-acting pyrazole contained in AI drugs.[12] A potent dual COX-2/5-LOX inhibitor, tepoxalin, demonstrates potent AI activity and is free of ulcerogenicity[13–15] (Figure 1).

Inspired by celecoxib, FPL 62064, and tepoxalin, new pyrazolone derivatives **3a**–**p** were synthesized by replacing the pyrazole moiety with a dihydropyrazolone nucleus, linked in C3 with 4-aminobenzoic acid or 4-aminobenzenesulfonamide. Moreover, position 4 of pyrazolone ring was substituted for a variety of chalcone derivatives, as it was reported that they have a promising effect in potentiating AI activity.[16,17] In addition, N1, either free or substituted for the phenyl ring, seemed to be important in interaction with the active site pocket of the COX-2 enzyme.

2 | RESULTS AND DISCUSSION

2.1 | Chemistry

Eighteen novel pyrazolone derivatives, **2a**,**b** and **3a**–**p**, were synthesized according to Scheme 1. The structure of the newly synthesized compounds was confirmed by infrared spectroscopy (IR), ^{1}H nuclear magnetic resonance spectroscopy (NMR), ^{13}C NMR spectral data, and elemental analyses. Firstly, key intermediates, **2a** and **2b**, were synthesized from 3-amino-pyrazol-5(4*H*)-one derivatives **1a** and **1b**, respectively, via heating under reflux with equimolar amounts of 4-aminobenzoic acid or sulfanilamide in water, acidified with hydrochloric acid, following the previously reported procedure.[18] ^{1}H NMR spectra showed that the derivatives **2a** and **2b** exist in two tautomeric forms. Compound **2a** exists as tautomers **A** and **B**, while compound **2b** exists in tautomeric forms **A** and **C** (Figure 2). This observation was consistent with the previously published work.[19,20] Examining the integration pattern of the ^{1}H NMR spectra throughout compounds **2a** and **2b** proved that tautomer **A** was more stable, as it was the major one in ^{1}H NMR spectra. The ^{1}H NMR spectrum of derivative **2a** revealed the presence of two singlet signals at δ: 3.46 (methylene protons), corresponding to tautomer **A** with integration as 2H and δ: 5.08 ppm (C=CH protons), corresponding to tautomer **B** with integration as 0.66H. Moreover, the aromatic protons of tautomer **A** appeared as two doublet signals at δ: 7.55 and 7.84 ppm, each, with the integration of 2H, while the aromatic protons of tautomer **B** appeared at δ: 7.22 and 7.74 ppm, each, with the integration of 1.3H. Finally, an extra D_2O exchangeable peak appeared at δ: 8.74 ppm with integration of 0.66H; which was another evidence of the presence of tautomer **B**. ^{13}C NMR also supported the presence of a tautomeric mixture with the appearance of an additional signal at 77.65 ppm, corresponding to methylidene carbon of tautomer **B**. In contrast, the ^{1}H NMR spectrum of compound **2b** showed the presence of signals at δ: 3.59 ppm (methylene protons), corresponding to tautomer **A**, with integration as 2H, and δ: 6.69 ppm (C=CH protons) corresponding to tautomer **C**, with integration as 0.42H. An additional D_2O exchangeable singlet at δ: 9.85 ppm, with integrations as 0.42H, corresponding to OH group in tautomer **C** was observed.

However, arylidene derivatives **3a**–**p** were prepared by reaction of the active methylene group of pyrazolone derivatives **2a** and **2b**, respectively, with different aromatic aldehydes, in the presence of a catalytic amount of anhydrous sodium acetate. The reaction is proposed to proceed via Knoevenagel reaction.[21,22]

The ^{1}H NMR spectra of **3a**–**p** showed characteristic disappearance of peaks, due to the methylene protons of **2a** and **2b**, and appearance of peaks of C=CH proton of arylidene, in the range of δ: 6.50–7.62 ppm, plus an increased number of protons

SCHEME 1 The synthetic pathway and reagents for the preparation of target compounds **2a**,**b** and **3a**–**p**. Reagents and conditions: (a) H_2O, reflux, 3 hr; (b) aromatic, glacial acetic acid, reflux, 5 hr

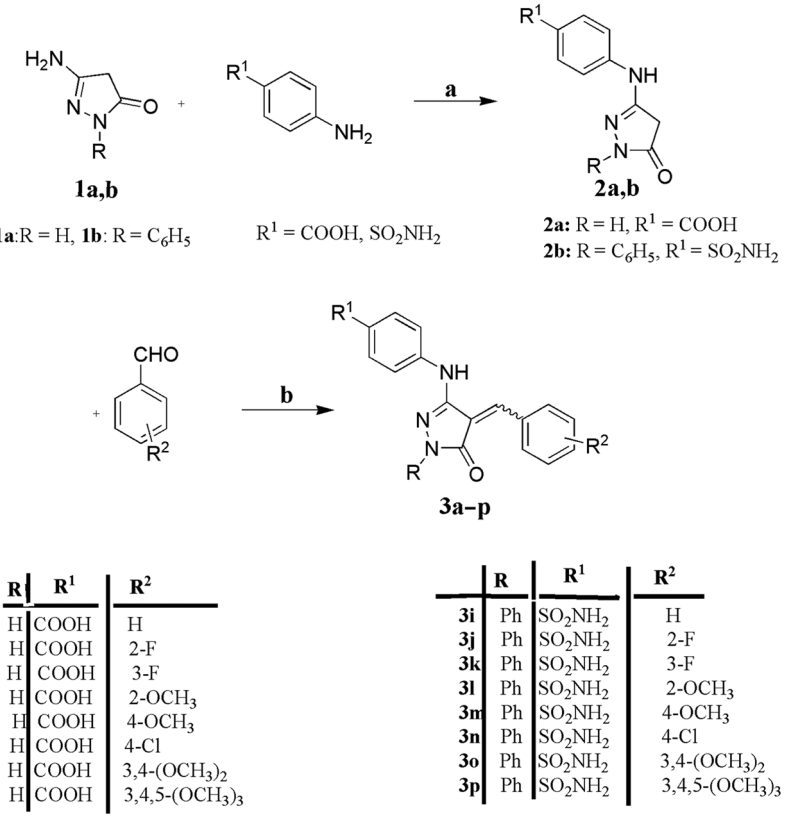

	R	R^1	R^2
3a	H	COOH	H
3b	H	COOH	2-F
3c	H	COOH	3-F
3d	H	COOH	2-OCH_3
3e	H	COOH	4-OCH_3
3f	H	COOH	4-Cl
3g	H	COOH	3,4-$(OCH_3)_2$
3h	H	COOH	3,4,5-$(OCH_3)_3$

	R	R^1	R^2
3i	Ph	SO_2NH_2	H
3j	Ph	SO_2NH_2	2-F
3k	Ph	SO_2NH_2	3-F
3l	Ph	SO_2NH_2	2-OCH_3
3m	Ph	SO_2NH_2	4-OCH_3
3n	Ph	SO_2NH_2	4-Cl
3o	Ph	SO_2NH_2	3,4-$(OCH_3)_2$
3p	Ph	SO_2NH_2	3,4,5-$(OCH_3)_3$

belonging to the aromatic system, at the expected chemical shifts and integral values. The ^{13}C NMR spectra of compounds **3a**–**p** showed peak disappearance of CH_2 of **2a** and **2b**, with the appearance of methylidene carbon at the range of δ: 136.50–147.27 ppm, and increase of aromatic carbons.

2.2 | Biological evaluation

2.2.1 | In vitro COX-1, COX-2, and 5-LOX enzyme inhibition assays

As compounds containing pyrazolone moiety are known to have AI activity,[23,24] the structure of the new derivatives **3a**–**p** is designed following the structure of celecoxib.[25] All the newly synthesized compounds **2a**,**b** and **3a**–**p** are evaluated for in vitro COX-1/COX-2 and 5-LOX inhibition assays, using both celecoxib

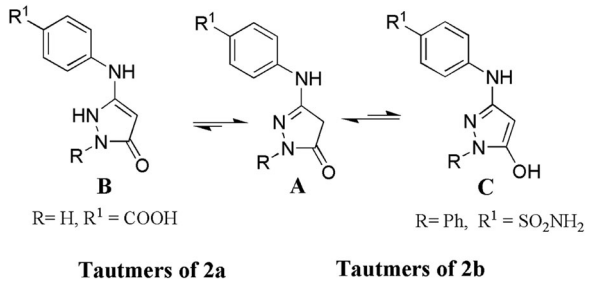

FIGURE 2 Tautomeric structures of compounds **2a**,**b**

and zileuton, as reference drugs, respectively. The compounds' activities are measured as concentration causing 50% enzyme activity inhibition (IC_{50}) and the selectivity index is calculated as IC_{50} (COX-1)/IC_{50} (COX-2). The results are summarized and represented graphically (Table 1 and Figures 3 and 4).

Compounds **3a**, **3e**, **3f**, **3h**, **3k**, **3l**, **3m**, **3n**, and **3p** showed clear preferential COX-2 over COX-1 inhibition, with remarkable SIs (2.46, 4.77, 11.69, 8.29, 3.74, 13.75, 3.24, 6.64, and 121.79, respectively), 1.24- to 61.82-fold higher than celecoxib (1.98). The selectivity index results showed that the substitution pattern of the pyrazolone ring was a crucial element for COX-2 selectivity. Substitution at C4 for trimethoxybenzylidene in compounds (**3h**, **3p**) greatly improved COX-2 selectivity and afforded most prominent compounds (4.21-, 61.82-fold, respectively, more selective than celecoxib), compared with the corresponding monomethoxy or monochloro derivatives, **3e**, **3f**, **3l**, **3m**, which were 2.40-, 5.90-, 6.95-, and 1.63-fold more selective than celecoxib. This observation was consistent with previously published work, reporting that substitution for trimethoxy groups increased the AI activity.[16] In contrast, the grafting phenyl group in position 1 of the pyrazolone ring and the presence of sulfonamide (SO_2NH_2) moiety, the most important pharmacophore for COX-2 selectivity,[26,27] significantly improved the activity, especially in compounds **3l** and **3p**, which may explain its maximum selectivity against COX-2. These results revealed that the bulkier derivatives showed better selectivity than the less bulky one based on that COX-2 enzyme, which showed a larger pocket than COX-1.[28] According to data

TABLE 1 In vitro COX-1, COX-2, selectivity index and 5-LOX enzyme inhibition assays of the synthesized compounds

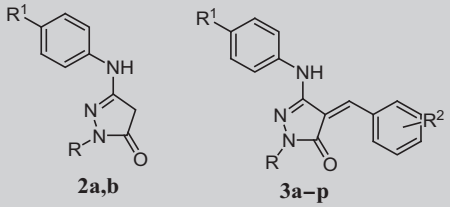

Compound no.	COX-1 IC_{50} (nM)[a]	COX-2 IC_{50} (nM)[a]	SI[b]	5-LOX IC_{50} (μM)[a]
Celecoxib	187.88 ± 13.2	95.02 ± 3.89	1.98	0.49 ± 0.01
Zileuton	ND	ND	ND	0.77 ± 0.03
2a	542.20 ± 17.2	965.80 ± 36.2	0.56	8.32 ± 0.29
2b	362.90 ± 13.9	647.01 ± 24.6	0.56	1.09 ± 0.04
3a	738.80 ± 3.14	299.80 ± 12.4	**2.46**	**0.60 ± 0.04**
3b	171.80 ± 6.1	160.70 ± 6.52	1.07	**0.70 ± 0.02**
3c	712.70 ± 22.4	1,018.63 ± 41.7	0.69	5.43 ± 0.26
3d	274.02 ± 13.5	499.10 ± 32.1	0.54	**0.79 ± 0.04**
3e	2,231 ± 34.7	467.26 ± 16.2	**4.77**	**1.30 ± 0.05**
3f	1,010.50 ± 29.2	**86.38 ± 4.71**	**11.69**	**0.67 ± 0.02**
3g	580.90 ± 17.3	635.28 ± 26.3	1.09	**0.64 ± 0.02**
3h	802.80 ± 31.4	**96.76 ± 5.1**	**8.29**	**1.45 ± 0.06**
3i	663.41 ± 22.4	1,130.22 ± 38.1	0.59	2.92 ± 0.08
3j	318.75 ± 12.1	341.59 ± 12.4	0.93	**0.46 ± 0.02**
3k	3,448.40 ± 127	922.59 ± 39.1	**3.74**	14.73 ± 0.64
3l	8,286.74 ± 274	**602.46 ± 12.7**	**13.75**	**1.08 ± 0.03**
3m	1,857.62 ± 76	572.33 ± 12.4	**3.24**	3.28 ± 0.11
3n	10,752.86 ± 314	1,617.05 ± 66.3	**6.64**	19.47 ± 0.84
3o	581.83 ± 21.2	1,925.82 ± 69.4	0.30	**0.92 ± 0.04**
3p	1,2081.05 ± 652	**99.19 ± 3.43**	**121.79**	**2.17 ± 0.09**

Note: The bold text indicates the compounds that are most selective for COX-2 enzyme and shows good 5-LOX inhibitory activity compared with celecoxib and zileuton as reference drugs.

Abbreviations: ND, not determined; SD, standard deviation; SE, standard error; SI, selectivity index.

[a]IC_{50} value is the concentration required to produce 50% inhibition of COX-1, COX-2, or 5-LOX for means of three determinations ± SD.

[b]In vitro COX-2 selectivity index = (IC_{50} of COX-1/COX-2).

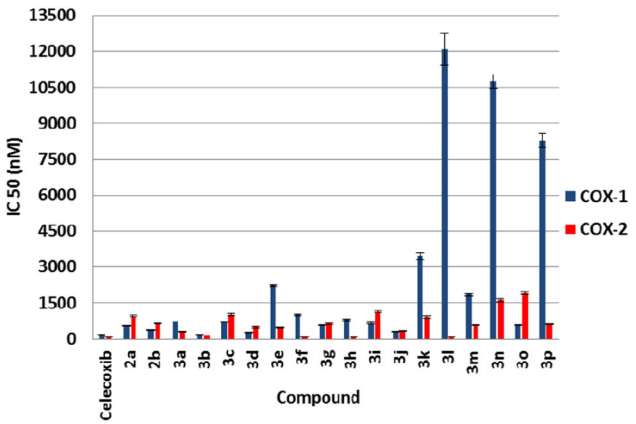

FIGURE 3 Graphical representation of IC_{50} (COX-1 and COX-2) values for the screened compounds in comparison with celecoxib

acquired from in vitro 5-lipoxygenase (5-LOX) inhibition assay, six compounds, **3d**, **3a**, **3b**, **3f**, **3g**, and **3j**, were the most promising derivatives, with IC_{50} of 0.79, 0.60, 0.70, 0.67, 0.64, and 0.46 μM. respectively. However, compounds, **3e**, **3h**, **3l**, **3o**, and **3p**, showed moderate 5-LOX inhibitory activity of IC_{50} values of 1.30, 1.45, 1.08, 0.92 and 2.17 μM, respectively, in comparison with zileuton (IC_{50} = 0.77 μM; Figure 4). The results of the 5-LOX inhibition assay revealed that disubstituted pyrazolone derivatives with monosubstituted phenyl moiety at C4 **3f** and **3e** have better 5-LOX inhibition than disubstituted pyrazolone derivatives with trimethoxyphenyl **3h** or trisubstituted one trimethoxyphenyl **3p**. The most promising compounds with the highest COX-2 inhibitory activity and excellent SIs, that is, **3f**, **3h**, **3l**, and **3p** were selected, for further in vivo pharmacological evaluation, using carrageenan-induced rat paw edema, gastrointestinal

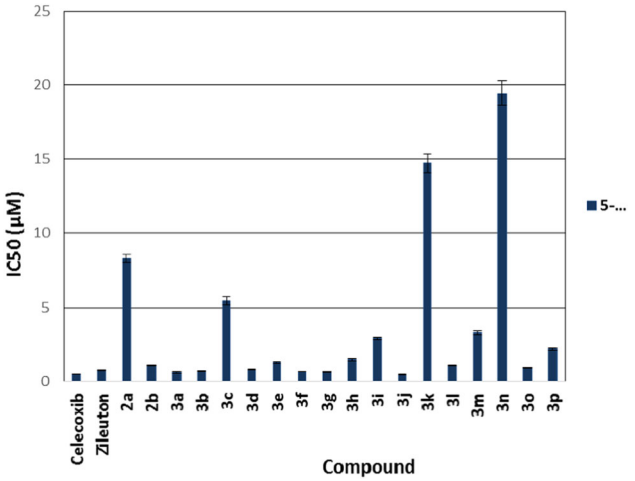

FIGURE 4 In vitro 5-LOX enzyme inhibition assay of the synthesized compounds in comparison with celecoxib

safety profile, and determination of rat serum prostaglandin E2 (PGE2).

2.2.2 | In vivo AI activity: Carrageenan-induced rat paw edema test

To explore the AI activity of the four most promising compounds, **3f**, **3h**, **3l**, and **3p**, which showed potential COX-2 and 5-LOX inhibition, they were further subjected to in vivo evaluation of their AI activity, using carrageenan-induced rat paw edema assay. The increase in rat paw volume and the ability of compounds to inhibit edema over a period of 4 hr were monitored, and the related results are displayed in Table 2.

Upon further examination of Table 2 and related results of statistical analysis, we were able to notice that all investigated compounds, **3f**, **3h**, **3l**, and **3p**, induced inhibition of edema percentage in the range of 34–46%, with AI activity almost better or identical to those of the reference standard agents, celecoxib (44%) or indomethacin (45%).

2.2.3 | Gastric ulcerogenic activity

Destruction of gastric mucosa is one of the most common adverse effects of chronic administration of NSAIDs. Therefore, the gastric ulcerogenic potential of compounds **3f**, **3h**, **3l**, and **3p** was estimated, upon oral administration. To figure out the ulcerogenic effects of tested compounds, rat intestinal mucosa was macroscopically observed for the presence of lesions, after oral administration of 10 mg/kg of said compounds, as well as of reference compounds (celecoxib and indomethacin). Isolated rat stomachs showed no ulceration, which was correlated with their selective COX-2 inhibitory profile in vitro, implying their gastric safety profile (Table 3).

2.2.4 | Determination of rat serum PGE2

The determination of serum PGE2 is a crucial parameter to evaluate the AI properties of the newly synthesized compounds. Being a chief inflammatory mediator, the reduction of PGE2 production in serum may contribute to the overall activity of the compounds. The same active compounds in the previous assay, **3f**, **3h**, **3l**, and **3p**, were subjected to evaluation of PGE2 in rat serum. The results show that they have good inhibition in PGE2 production, **3f** (57%), **3h** (66%), **3l** (54%), and **3p** (54%), in comparison with celecoxib (70%) and indomethacin (73%), as shown in Table 4.

Accordingly, these results show good connection between the selective activity on COX-2 enzyme and the reduction in serum PGE2 production as one of the main inflammatory mediators produced through the COX-2 enzyme pathway.

TABLE 2 In vivo carrageenan-induced rat paw edema assay increase in rat paw volume and percentage of edema inhibition

	Average increase in paw volume (ml^3) ± SE					% Edema inhibition				
	Time (hr)									
Compound	0	1	2	3	4	0	1	2	3	4
Control	0.72 ± 0.03	1.11 ± 0.05	1.98 ± 0.14	2.61 ± 0.85	2.97 ± 0.15	NA	NA	NA	NA	NA
3f	0.81 ± 0.08	1.45 ± 0.04	1.89 ± 0.03*	2.15 ± 0.08*	1.95 ± 0.05*	NA	NA	6	23	34
3h	0.67 ± 0.05	0.91 ± 0.07	1.58 ± 0.07*	1.77 ± 0.06*	1.68 ± 0.06*	7	7	13	30	46
3l	0.72 ± 0.05	0.98 ± 0.06	1.71 ± 0.06*	1.86 ± 0.04*	1.67 ± 0.09*	NA	3	12	27	45
3p	0.68 ± 0.05	1.02 ± 0.06	1.79 ± 0.04*	1.96 ± 0.08*	1.85 ± 0.04*	NA	NA	7	24	39
Celecoxib	0.68 ± 0.05	0.97 ± 0.06	1.69 ± 0.07*	1.78 ± 0.04*	1.67 ± 0.05*	7	7	13	30	44
Indomethacin	0.68 ± 0.05	0.95 ± 0.07	1.63 ± 0.02*	1.71 ± 0.05*	1.68 ± 0.06*	4	7	16	33	45

Note: Data are expressed as mean ± SE. Statistical analysis of the data was done using one-way analysis of variance. Probability levels of $p < 0.05$ were considered statistically significant.

*Significantly different from the control group ($p < 0.05$).

TABLE 3 Gastric ulcerative effect of tested compounds **3f**, **3h**, **3j**, **3l**, and **3p** compared with celecoxib and indomethacin in male albino rats ($n = 6$)

	Score	
Groups	No. of gastric ulcers	Severity lesions
Control (1 ml saline)	0	0
3f	0	0
3h	0	0
3l	0	0
3p	0.1	0
Celecoxib	0	0
Indomethacin	5	5

2.3 | Molecular docking in the COX-2 and 5-LOX active sites

The binding site of the COX-2 enzyme possesses an additional secondary pocket, which is absent in the COX-1 enzyme. This secondary pocket is attributed to the replacement of amino acid Ile532 in COX-1 with less bulky Val532 in COX-2.[29] Hence, selective COX-2 inhibitors usually contain bulky rigid groups (such as sulfonamide or di-, trisubstituted phenyl) that allow for additional binding interactions inside COX-2 secondary pocket and prevent the compound from fitting inside the narrower COX-1 channel. This additional binding interaction of the inhibitor is thought to be responsible for the selectivity of COX-2 inhibitors.[25,27] Furthermore, interactions with Arg513, which is replaced by His513 in COX-1, are also thought to be crucial for the selectivity.[30] Therefore, to elucidate the possible interactions of the most active compounds **3f**, **3h**, **3l**, and **3p** with either COX-2 (PDB entry 1CX2) or 5-LOX (PDB entry 3V99) receptors, a molecular docking study was carried out using Molecular Operating Environment (MOE; version 2008.10) modeling software.[26,31] Docking scores and binding interactions inside COX-2 and 5-LOX active sites are summarized in Table 5.

Regarding the COX-2 enzyme, the energy-scoring functions, hydrogen bonds formed with the surrounding amino acids and the orientation of the docked compounds with respect to the cocrystallized ligand SC-558 and celecoxib were used to evaluate the binding affinities to the active site of COX-2. The docking protocol itself was validated through the redocking of the cocrystallized structure of the reference ligand (SC-558). Then, the docking results were compared with that of the crystallized reference ligand. This comparison was carried out by calculating root mean square deviation (RMSD), and an RMSD of 0.6363 Å was found, with an energy score of −14.84 kcal/mol. The docking study of compounds **3f**, **3h**, **3l**, and **3p** showed energy scores of −14.32, −17.12, −16.40 and −20.71 kcal/mol, respectively, which are almost better affinities than SC-558 and celecoxib toward the COX-2 active site. The phenylsulfonamide ring of the reference ligand and celecoxib occupies the additional secondary pocket observed in the COX-2 enzyme, where the sulfonamide oxygen showed interactions with two key amino acids His90 and Arg513 (Figure 5).

TABLE 4 In vivo determination of rat serum PGE2

Compound	PGE2, mean serum conc. (pg/ml)	Inhibition (%)
Control (pre-carrageenan)	110.72 ± 6.12	NA
Control 1 (post-carrageenan)	677.41 ± 7.22	NA
3f	287.67 ± 7.89	57
3h	228.68 ± 7.21*	66
3l	205.76 ± 7.21*	69
3p	305.21 ± 6.92*	54
Celecoxib	199.89 ± 8.41*	70
Indomethacin	182.65 ± 9.72*	73

*Significant from Control group 1 (post-carrageenan).

Interestingly, compounds **3f** and **3l** showed the same binding pattern with the same amino acids as the standard drug, as they formed a hydrogen bond with His90 using the carboxylate group and sulfonamide group, respectively; additionally, they showed a hydrogen bond and arene–cation interaction with Arg513. Moreover, compound **3f** showed extra arene–cation interaction with Arg120, which had a role in COX-2 inhibitory activity[32] (Figures 6 and 7).

In a different way, compounds **3h** and **3p** shared an interesting common feature, where the methoxy groups interacted as a H-bond acceptor with the amino acid Ser530. Interactions with Ser530 have been reported to play important roles in the inhibition of COX-2 enzyme by diaryl heterocyclic compounds.[32,33] Moreover, they showed the highest energy score, −17.12 and −20.71 kcal/mol, respectively. This might have been due to extra hydrogen bonds formed with Gln192, Leu352, Tyr355, and Tyr385 (Figures 8 and 9). Tyr385 is an important key amino acid residue at the COX-2 binding site.[34]

An overlay of the docking poses of compounds **3f**, **3h**, **3l**, and **3p** showed perfect superimposition with respect to the reference drug SC-558 (Figures 6, 7, 8, and 9). This correlated well with the ability of these compounds to fit in the COX-2 active site, and hence, to display remarkable COX-2 inhibitory activity and selectivity.

As for 5-LOX enzyme, zileuton belonged to the group of chelating inhibitors of the 5-LOX, chelating the active iron (Fe) site of the enzyme.[35] The hydroxyl group of the hydroxyl urea part of zileuton showed metal interaction with Fe^{2+} region in the active site of 5-LOX enzyme, with an energy score of −6.3 kcal/mol (Figure 10). Moreover, it showed hydrogen bond interaction with Asn554, the important amino acid in the 5-LOX active site.[36] Compounds **3f** and **3h** made similar interactions with the Fe^{2+} region as that of zileuton. The proposed binding mode of compound **3h** inside the 5-LOX receptor active site is displayed in Figure 11.

TABLE 5 The docking scores and binding interactions of **3f**, **3h**, **3l**, and **3p** inside COX-2 and 5-LOX active sites

	COX-2				5-LOX			
Compound no.	Docking score (kcal/mol)	Amino acid	Functional group	Type of interaction	Docking score (kcal/mol)	Amino acid	Functional group	Type of interaction
SC-558	−14.84	His20	SO_2	H-bond	–	–	–	
		Arg513	SO_2	H-bond				
Celecoxib	−8.04	His20	SO_2	H-bond	–	–	–	
		Arg513	SO_2	H-bond				
Zileuton	–	–	–	–	−6.30		OH	Metal complex (Fe)
						Asn554	OH	H-bond
						Ala672	NH	H-bond
						Val672	NH	H-bond
3f	−14.32	His20	COO^-	H-bond	−7.20		COO^-	Metal complex (Fe)
		Arg513	COO^-	H-bond		Phe177	Pyrazole C=O	H-bond
		Arg120	Phenyl	Arene–cation		Phe177	Phenyl	Arene–cation
3h	−17.12	Tyr355	Pyrazole N-2	H-bond	−7.68		COO^-	Metal complex (Fe)
		Tyr355	NH	H-bond		Phe177	Pyrazole C=O	H-bond
		Tyr385	OCH_3	H-bond		Phe177	Phenyl	Arene–cation
		Ser530	OCH_3	H-bond				
3l	−16.40	His20	SO_2	H-bond	−6.46	Phe177	Pyrazole C=O	H-bond
		Arg513	Phenyl	Arene–cation		Asn554	SO_2	H-bond
		Gln192	NH	H-bond		Ala672	NH	H-bond
		Leu352	NH	H-bond				
3p	−20.71	Tyr355	Pyrazole N-2	H-bond	−6.82	Phe177	Pyrazole C=O	H-bond
		Tyr355	NH	H-bond		Phe177	Phenyl	Arene–cation
		Tyr385	OCH_3	H-bond		Asn554	SO_2	H-bond
		Ser530	OCH_3	H-bond		Ala672	NH	H-bond
		Gln192	NH	H-bond				
		Leu352	NH	H-bond				

3 | CONCLUSION

A new series of pyrazolone derivatives bearing benzoic acid or benzene sulfonamide were designed and synthesized, with the aim of finding new derivatives with AI activity, by inhibiting both COX-2 and 5-LOX enzymes, overcoming the side effects of other selective COX-2 inhibitors. In light of the pharmacological activity, compounds **3f**, **3h**, **3l**, and **3p** (22.22%) exhibited good activity toward the COX-2 enzyme. Moreover, it was shown that nine compounds (50%) showed clear preferential COX-2 over COX-1 inhibition with remarkable SIs, 11

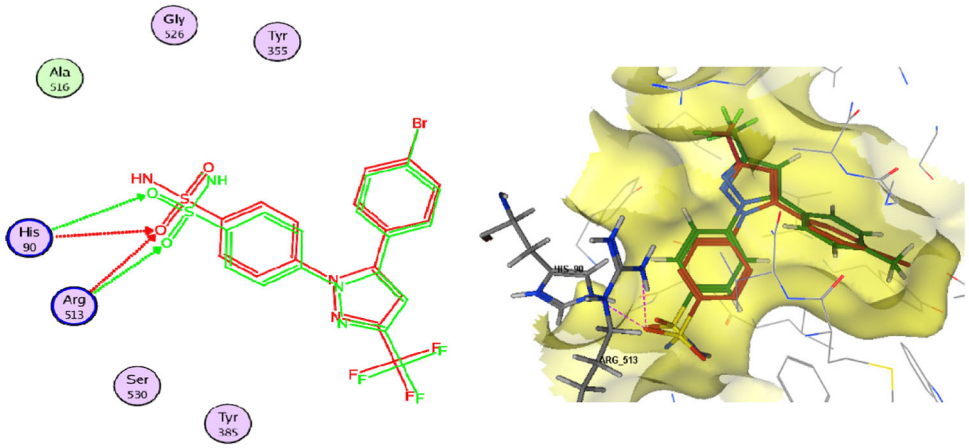

FIGURE 5 Docking and binding pattern of SC-558 (red) and celecoxib (violet) into COX-2 active site (PDB: 1CX2) in 2D (left panel) and 3D (right panel)

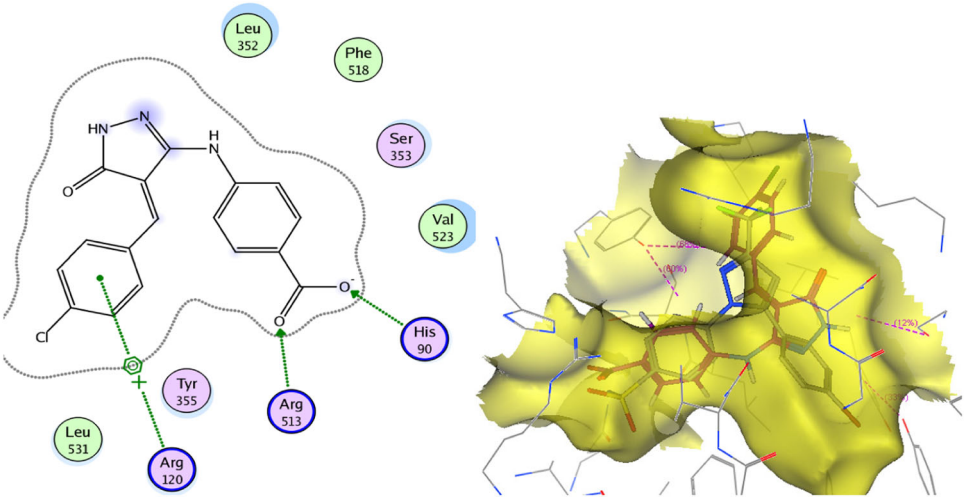

FIGURE 6 Docking and binding pattern of **3f** into COX-2 active site in 2D (left panel) and 3D (right panel)

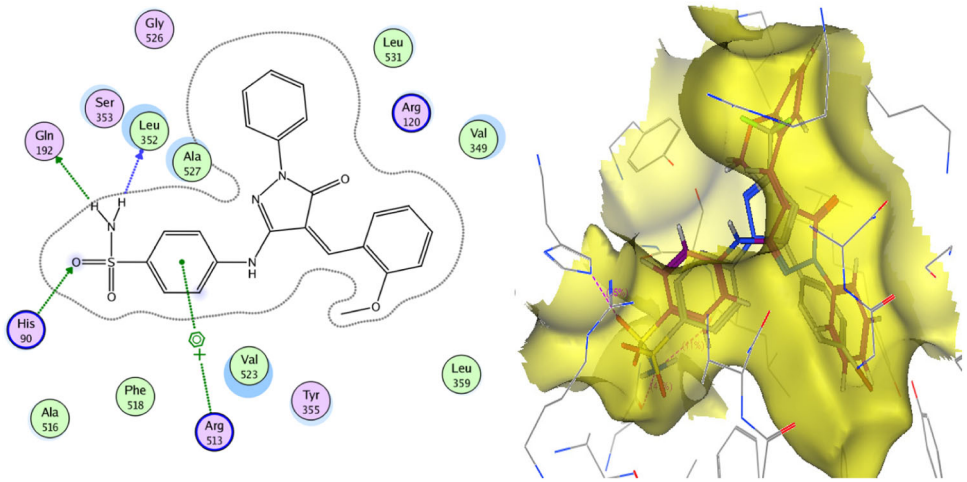

FIGURE 7 Docking and binding pattern of **3l** into COX-2 active site in 2D (left panel) and 3D (right panel)

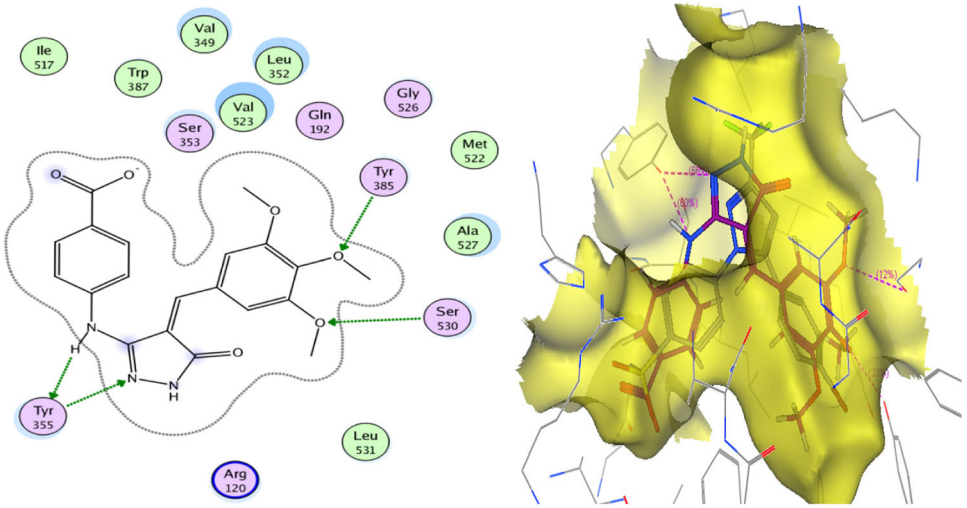

FIGURE 8 Docking and binding pattern of **3h** into COX-2 active site (PDB: 1CX2) in 2D (left panel) and 3D (right panel)

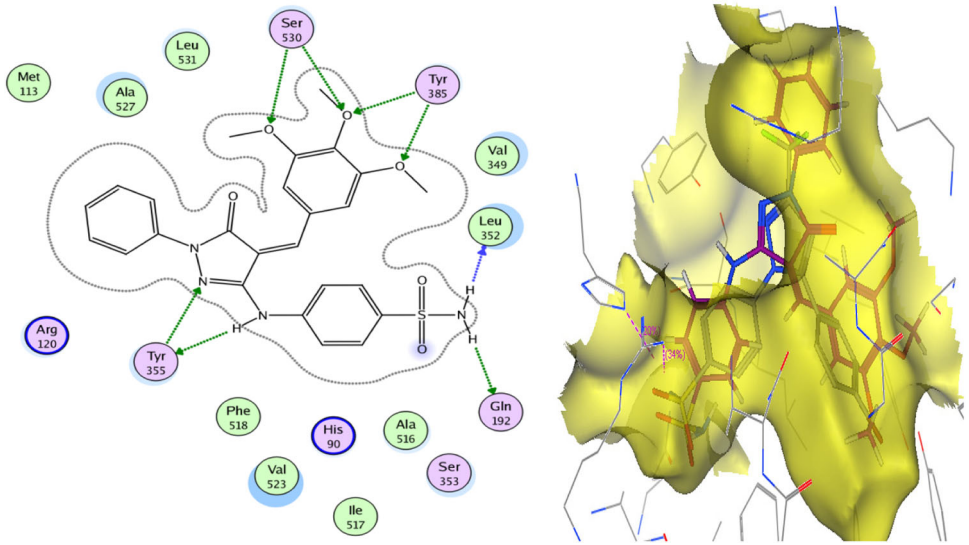

FIGURE 9 Docking and binding pattern of **3p** into COX-2 active site in 2D (left panel) and 3D (right panel)

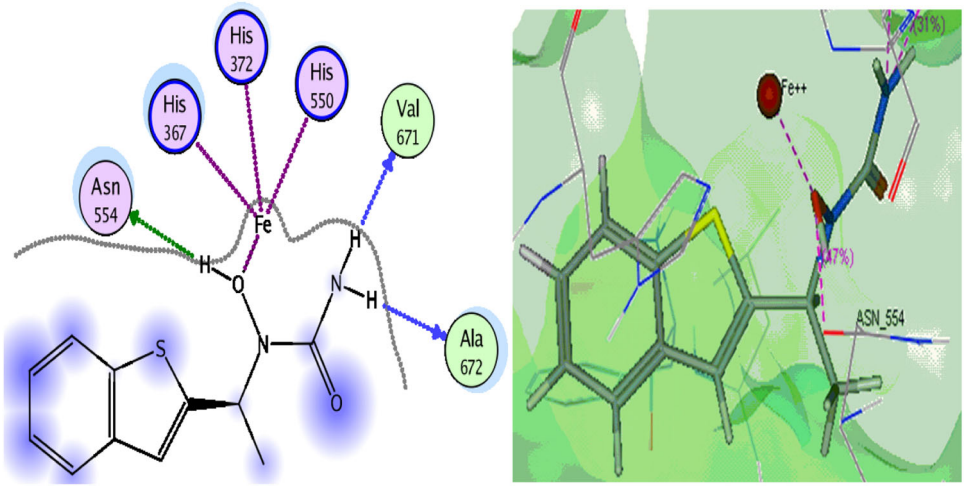

FIGURE 10 Docking and binding pattern of zileuton into 5-LOX active site (PDB: 3V99) in 2D (left panel) and 3D (right panel)

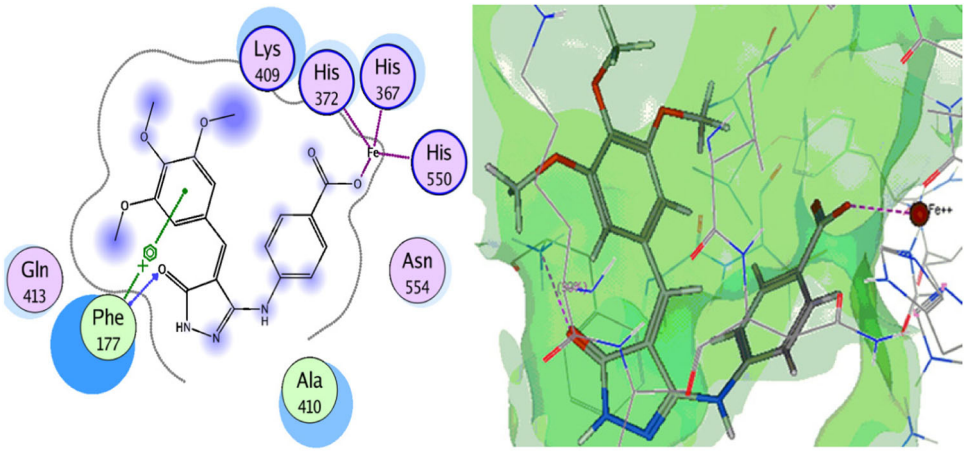

FIGURE 11 Docking and binding pattern of **3h** into 5-LOX active site in 2D (left panel) and 3D (right panel)

derivatives (61.11%) were good 5-LOX inhibitors, and 4 tested compounds (22.22%) were dual COX-2/5-LOX inhibitors. The four most active compounds, **3f**, **3h**, **3l**, and **3p**, were further screened in vivo and showed remarkable results, in comparison with celecoxib, as AI agents. The same compounds showed similar interaction to that of SC-558 and zileuton. Interestingly, these derivatives also decreased the production of PGE2, encouraging further future investigation for these derivatives, as they act on enzymes involved in both AA pathways.

4 | EXPERIMENTAL

4.1 | Chemistry

4.1.1 | General

Melting points were determined on Stuart apparatus and the values given were uncorrected. IR spectra were determined on a Shimadzu IR 435 spectrophotometer (Shimadzu Corp., Kyoto, Japan) at the Microanalytical Center, Faculty of Pharmacy, Cairo University, and values were represented in cm^{-1}. ^1H NMR spectra were investigated using a Bruker 400 MHz (Bruker Corp., Billerica, MA) spectrophotometer, at the Microanalytical Center, Faculty of Pharmacy, Cairo University, Egypt. Tetramethylsilane was used as internal standard and chemical shift values were recorded in ppm on δ scale and coupling constants (J) were given in Hz. ^{13}C NMR spectra were studied using a Bruker 100 MHz spectrophotometer, at the Microanalytical Center, Faculty of Pharmacy, Cairo University, Egypt. Microanalyses for C, H, and N were carried out at the Regional Center for Mycology and Biotechnology, Faculty of Pharmacy, Al Azhar University, Egypt. The progress of the reactions was monitored using TLC aluminum sheets precoated with UV fluorescent silica gel Merck 60 F254. The spots were visualized using a UV lamp.

The NMR spectra as well as the InChI codes of the investigated compounds together with some biological activities are provided as Supporting Information Data.

4.1.2 | Synthesis and procurement of compounds 1a,b

3-Amino-1*H*-pyrazol-5(4*H*)-one **1a** was synthesized according to the reported procedures[18] while 3-amino-1-phenyl-1*H*-pyrazol-5(4*H*)-one **1b** was commercially available from Fluka chemicals.

4.1.3 | General procedure for the synthesis of compounds 2a,b

To a solution of concentrated hydrochloric acid (10 ml) in water (100 ml), a mixture of 3-amino-pyrazol-5(4*H*)-one derivatives (**1a**,**b**; 0.1 mol) and 4-aminobenzoic acid (13.7 g, 0.1 mol) or sulfanilamide (17.2 g, 0.1 mol) was added, and the reaction mixture was heated under reflux for 3 hr. The solution was filtered while hot and the obtained white solid was washed with water, dried, and crystallized from ethanol.

*4-(4,5-Dihydro-5-oxo-1H-pyrazol-3-ylamino)benzoic acid (**2a**)*

Yield: 46%; white solid; m.p. 293–295°C; IR (KBr) cm^{-1}: 3,403 (OH), 3,317, 3,155 (NH), 3,095–3,024 (arom. CH), 2,924 (aliph. CH), 1,720, 1,695 (C═O), 1,593 (C═N); ^1H NMR (dimethylsulfoxide [DMSO]-d_6) δ ppm: 3.46 (s, 2H, CH_2), 5.08 (s, 0.66H, CH, taut. **B**), 7.22 (d, J = 8.6 Hz, 1.30H, arom. CH, taut. **B**), 7.55 (d, J = 8.6 Hz, 2H, arom. CH), 7.74 (d, J = 8.6 Hz, 1.30H, arom. CH, taut. **B**), 7.84 (d, J = 8.6 Hz, 2H, arom. CH), 8.74 (s, 0.65H, NH, D_2O exchangeable, taut. **B**), 9.58 (s, 1H, NH, D_2O exchangeable), 10.49 (s, 1H, NH, D_2O exchangeable), 11.67 (s, 2H, OH, D_2O exchangeable); ^{13}C NMR (DMSO-d_6) δ ppm: 37.50 (C4, pyrazole, CH_2), 77.65 (C4, pyrazole, CH_2, taut. **B**), 114.13 (C1, benzoic acid), 116.74 (C3,5, benzoic acid), 131.01 (C2,6, benzoic acid), 131.28 (C2,6, benzoic acid, taut. **B**), 144.70 (C4, benzoic acid), 148.22 (C4, benzoic acid, taut. **B**), 152.78 (C3, pyrazole), 168.11 (C═O, pyrazole), 171.59 (C═O, benzoic); anal. calcd. for $C_{10}H_9N_3O_3$ (219.06): C, 54.97; H, 4.11; N, 19.17; found C, 55.02; H, 4.26; N, 19.41.

*4-[(5-Oxo-1-phenyl-4,5-dihydro-1H-pyrazol-3-yl)amino] benzenesulfonamide (**2b**)*

Yield: 75%; pale yellow solid; m.p. 182–184°C; IR (KBr) cm^{-1}: 3,475, 3,375, 3,244 (NH), 3,051–3,066 (arom. CH), 2,912 (aliph. CH), 1,681 (C═O); ^1H NMR (DMSO-d_6) δ ppm: 3.59 (s, 2H, CH_2), 6.69 (s, 0.42H, CH, taut. **C**), 6.71–6.79 (m, 2H, arom. CH), 7.13–7.20 (m, 2H, arom. CH), 7.25 (s, 2H, SO_2NH_2, D_2O exchangeable), 7.42 (t, J = 7.9 Hz, 1H, arom. CH), 7.64 (d, J = 7.8 Hz, 2H, arom. CH), 7.78 (d, J = 8 Hz, 2H, arom. CH), 9.85 (s, 0.42H, OH, D_2O exchangeable, taut. **C**), 10.50 (s, 1H, NH, D_2O exchangeable), 11.42 (s, 1H, NH, D_2O exchangeable); ^{13}C NMR (DMSO-d_6) δ ppm: 38.17 (C4, pyrazole), 112.65 (C3,5, benzenesulfonamide), 118.95 (C2,6, phenyl), 125.07 (C4, phenyl), 127.23 (C2,6, benzenesulfonamide), 129.14 (C1, benzenesulfonamide), 129.31 (C3,5, phenyl), 138.99 (C1, phenyl), 142.21 (C4, benzenesulfonamide), 149.42 (C3, pyrazole), 166.69 (C═O, pyrazole); anal. calcd. for $C_{15}H_{14}N_4O_3S$ (330.08): C, 54.53; H, 4.27; N, 16.96; found C, 54.80; H, 4.41; N, 16.78.

4.1.4 | General procedure for the synthesis of compounds 3a–p

To a solution of an appropriate compound **2a**,**b** (0.001 mol) in acetic acid (10 ml) buffered with sodium acetate (0.08 g, 0.001 mol), aromatic aldehyde derivatives (0.001 mol) were added. The mixture was refluxed for 8 hr, cooled and then poured into water. The precipitate was filtered, washed with water, and crystallized from ethanol.

*4-((4Z)-4-Benzylidene-4,5-dihydro-5-oxo-1H-pyrazol-3-ylamino) benzoic acid (**3a**)*

Yield: 60%; buff solid; m.p. 223–225°C; IR (KBr) cm^{-1}: 3,390 (OH), 3,197, 3,116 (NH), 3,035–3,062 (arom. CH), 1,720, 1,693 (C═O), 1,593 (C═N); ^1H NMR (DMSO-d_6) δ ppm: 7.13–8.52 (m, 10H, C═CH, and arom. CH),

9.18 (s, 1H, NH, D_2O exchangeable), 10.03 (s, 1H, NH, D_2O exchangeable), 12.09 (s, 1H, OH, D_2O exchangeable); ^{13}C NMR (DMSO-d_6) δ ppm: 114.08 (C3,5, benzoic), 116.66 (C1, benzoic), 127.39 (C4, pyrazole), 127.89 (C2,6, benzene), 128.48 (C4, benzene), 129.67 (C3,5, benzene), 131.02 (C2,6, benzoic), 135.12 (C1, benzene), 144.53 (methylidene carbon), 148.27 (C4, benzoic), 152.80 (C1, pyrazole), 168.65 (C=O, pyrazole), 169.06 (C=O, benzoic); anal. calcd. for $C_{17}H_{13}N_3O_3$ (307.1): C, 66.44; H, 4.23; N, 13.68; found C, 66.71; H, 4.39; N, 13.89.

*4-[(4Z)-4-(2-Fluorobenzylidene)-4,5-dihydro-5-oxo-1*H*-pyrazol-3-ylamino]benzoic acid (**3b**)*

Yield: 73%; brick red solid, m.p. >300°C; IR (KBr) cm^{-1}: 3,387 (OH), 3,217, 3,197 (NH), 3,032–3,062 (arom. CH), 1,705, 1,681 (C=O), 1,604 (C=N); ^1H NMR (DMSO-d_6) δ ppm: 6.88 (s, 1H, C=CH), 7.04–7.08 (m, 2H, arom. CH), 7.22 (t, J = 7.8 Hz, 1H, arom. CH), 7.54 (t, J = 7.6 Hz, 1H, arom. CH), 7.65 (d, J = 8.7 Hz, 1H, arom. CH), 7.78 (d, J = 8.6 Hz, 2H, arom. CH), 7.91 (d, J = 8.3 Hz, 1H, arom. CH), 8.15 (d, J = 8.3, 1H, arom. CH), 8.73 (s, 1H, NH, D_2O exchangeable), 11.09 (s, 1H, NH, D_2O exchangeable), 12.32 (s, 1H, OH, D_2O exchangeable); ^{13}C NMR (DMSO-d_6) δ ppm: 113.58 (C3, benzene), 116.51 (C3,5, benzoic), 117.41 (C1, benzoic), 119.70 (C1, benzene), 120.73 (C5, benzene), 123.66 (C4, pyrazole), 128.29 (C6, benzene), 130.98 (C4, benzene), 131.74 (C2,6, benzoic), 147.27 (methylidene carbon), 148.91 (C4, benzoic), 151.80 (C3, pyrazole), 153.55 (C2, benzene), 167.68 (C=O, pyrazole), 167.84 (C=O, benzoic); anal. calcd. for $C_{17}H_{12}FN_3O_3$ (325.09): C, 62.76; H, 3.69; N, 12.92; found C, 62.59; H, 3.83; N, 13.14.

*4-[(4Z)-4-(3-Fluorobenzylidene)-4,5-dihydro-5-oxo-1*H*-pyrazol-3-ylamino]benzoic acid (**3c**)*

Yield: 67%; brown solid; m.p. 254–256°C; IR (KBr) cm^{-1}: 3,407 (OH), 3,317, 3,201 (NH), 3,021–3,078 (arom. CH), 1,720, 1,697 (C=O), 1,593 (C=N); ^1H NMR (DMSO-d_6) δ ppm: 6.62–8.23 (m, 9H, C=CH, and arom. CH), 9.23 (s, 1H, NH, D_2O exchangeable), 11.09 (s, 1H, NH, D_2O exchangeable), 12.10 (s, 1H, OH, D_2O exchangeable); ^{13}C NMR (DMSO-d_6) δ ppm: 110.06 (C2, benzene), 113.90 (C4, benzene), 117.20 (C3,5, benzoic), 120.72 (C1, benzoic), 123.24 (C6, benzene), 124.40 (C4, pyrazole), 129.46 (C5, benzene), 131.00 (C2,6, benzoic), 135.49 (C1, benzene), 143.36 (methylidene carbon), 144.04 (C4, benzoic), 152.90 (C3, pyrazole), 163.12 (C3, benzene), 167.54 (C=O, pyrazole), 170.01 (C=O, benzoic); anal. calcd. for $C_{17}H_{12}FN_3O_3$ (325.09): C, 62.76; H, 3.69; N, 12.92; found C, 62.84; H, 3.90; N, 13.21.

*4-[(4Z)-4-(2-Methoxybenzylidene)-4,5-dihydro-5-oxo-1*H*-pyrazol-3-ylamino]benzoic acid (**3d**)*

Yield: 63%; buff solid; m.p. 248–250°C; IR (KBr) cm^{-1}: 3,387 (OH), 3,278, 3,201 (NH), 3,074–3,008 (arom. CH), 2,839 (aliph. CH), 1,718, 1,697 (C=O), 1,597 (C=N); ^1H NMR (DMSO-d_6) δ ppm: 3.93 (s, 3H, OCH_3), 6.82–8.29 (m, 9H, C=CH, and arom. CH), 9.33 (s, 1H, NH, D_2O exchangeable), 10.84 (s, 1H, NH, D_2O exchangeable), 12.47 (s, 1H, OH, D_2O exchangeable); ^{13}C NMR (DMSO-d_6) δ ppm: 56.38 (OCH_3), 111.61 (C3, benzene), 116.27 (C1, benzene), 117.14 (C3,5, benzoic), 120.17 (C1, benzoic), 121.90 (C5, benzene), 127.47 (C4, pyrazole), 130.97 (C2,6, benzoic), 131.29 (C4,6, benzene), 145.70 (methylidene carbon), 149.80 (C4, benzoic), 157.32 (C3, pyrazole), 163.19 (C2, benzene), 167.32 (C=O, pyrazole), 167.59 (C=O, benzoic); anal. calcd. for $C_{18}H_{15}N_3O_4$ (337.11): C, 64.09; H, 4.45; N, 12.46; found C, 64.35; H, 4.61; N, 12.72.

*4-[(4Z)-4-(4-Methoxybenzylidene)-4,5-dihydro-5-oxo-1*H*-pyrazol-3-ylamino]benzoic acid (**3e**)*

Yield: 78%; brown solid; m.p. 236–238°C; IR (KBr) cm^{-1}: 3,405 (OH), 3,197, 3,120 (NH), 3,074–3,008 (arom. CH), 2,935 (aliph. CH), 1,720, 1,681 (C=O), 1,589 (C=N); ^1H NMR (DMSO-d_6) δ ppm: 3.87 (s, 3H, OCH_3), 6.81 (s, 1H, C=CH), 7.12 (d, J = 8.4 Hz, 2H, arom. CH), 7.65 (d, J = 7.9 Hz, 2H, arom. CH), 7.88 (d, J = 8.3 Hz, 2H, arom. CH), 8.63 (d, J = 8.48 Hz, 2H, arom. CH), 9.08 (s, 1H, NH, D_2O exchangeable), 10.88 (s, 1H, NH, D_2O exchangeable), 12.17 (s, 1H, OH, D_2O exchangeable); ^{13}C NMR (DMSO-d_6) δ ppm: 56.08 (OCH_3), 114.75 (C3,5, benzene), 116.95 (C3,5, benzoic), 119.31 (C1, benzoic), 126.44 (C4, pyrazole), 131.00 (C2,6, benzene), 136.62 (C2,6, benzoic), 144.6 (methylidene carbon), 145.58 (C4, benzoic), 148.02 (C3, pyrazole), 163.46 (C4, benzene), 163.72 (C=O, pyrazole), 167.87 (C=O, benzoic); anal. calcd. for $C_{18}H_{15}N_3O_4$ (337.11): C, 64.09; H, 4.45; N, 12.46; found C, 64.31; H, 4.69; N, 12.65.

*4-[(4Z)-4-(4-Chlorobenzylidene)-4,5-dihydro-5-oxo-1*H*-pyrazol-3-ylamino]benzoic acid (**3f**)*

Yield: 68%; buff solid; m.p. 241–243°C; IR (KBr) cm^{-1}: 3,402 (OH), 3,305, 3,201 (NH), 3,109–3,054 (arom. CH), 1,720, 1,697 (C=O), 1,593 (C=N); ^1H NMR (DMSO-d_6) δ ppm: 6.81 (s, 1H, C=CH), 7.01–7.44 (m, 5H, arom. CH), 7.65–8.04 (m, 3H, arom. CH), 9.97 (s, 1H, NH, D_2O exchangeable), 10.87 (s, 1H, NH, D_2O exchangeable), 12.09 (s, 1H, OH, D_2O exchangeable); ^{13}C NMR (DMSO-d_6) δ ppm: 114.37 (C3,5, benzoic), 117.59 (C1, benzoic), 128.38 (C4, pyrazole), 128.62 (C2,6, benzene), 129.17 (C3,5, benzene), 131.06 (C2,6, benzoic), 131.65 (C1,4, benzene), 142.31 (methylidene carbon), 150.44 (C4, benzoic), 155.40 (C3, pyrazole), 167.77 (C=O, pyrazole), 172.53 (C=O, benzoic); anal. calcd. for $C_{17}H_{12}ClN_3O_3$ (341.06): C, 59.73; H, 3.51; N, 12.29; found C, 60.02; H, 3.67; N, 12.04.

*4-[(4Z)-4-(3,4-Dimethoxybenzylidene)-4,5-dihydro-5-oxo-1*H*-pyrazol-3-ylamino]benzoic acid (**3g**)*

Yield: 77%; brick red solid; m.p. 233–235°C; IR (KBr) cm^{-1}: 3,408 (OH), 3,263, 3,197 (NH), 3,078–3,005 (arom. CH), 2,939 (aliph. CH), 1,720, 1,693 (C=O), 1,589 (C=N); ^1H NMR (DMSO-d_6) δ ppm: 3.73 (s, 3H, OCH_3), 3.89 (s, 3H, OCH_3), 6.68 (s, 1H, C=CH), 7.02 (d, J = 8.4 Hz, 1H, arom. CH), 7.16 (d, J = 8 Hz, 1H, arom. CH), 7.23 (t, 1H, J = 7.3 Hz arom. CH), 7.72 (d, J = 8.5 Hz, 2H, arom. CH), 7.88 (d, J = 8.5 Hz, 2H, arom. CH), 9.07 (s, 1H, NH, D_2O exchangeable), 10.88 (s, 1H, NH, D_2O exchangeable), 12.05 (s, 1H, OH, D_2O exchangeable); ^{13}C NMR (DMSO-d_6) δ ppm: 55.73 (OCH_3), 55.93 (OCH_3), 111.73 (C2, benzene), 116.14 (C5, benzene), 117.01 (C3,5, benzoic), 119.08 (C6, benzene), 122.59 (C1, benzoic), 125.74 (C4, pyrazole), 128.64 (C1, benzene), 129.34 (C2,6, benzoic), 137.82 (methylidene carbon), 147.40 (C4, benzene), 148.13 (C4, benzoic), 148.64 (C3, benzene), 153.52 (C3, pyrazole), 163.86 (C=O, pyrazole), 167.72 (C=O,

benzoic); anal. calcd. for $C_{19}H_{17}N_3O_5$ (367.12): C, 62.12; H, 4.63; N, 11.44; found C, 62.30; H, 4.84; N, 11.57.

*4-[(4Z)-4-(3,4,5-Trimethoxybenzylidene)-4,5-dihydro-5-oxo-1H-pyrazol-3-ylamino]benzoic acid (**3h**)*

Yield: 81%; brown solid; m.p. 200–202°C; IR (KBr) cm^{-1}: 3,413 (OH), 3,263, 3,194 (NH), 3,051–3,005 (arom. CH), 2,839 (aliph. CH), 1,720, 1,693 (C=O), 1,593 (C=N); ^{1}H NMR (DMSO-d_6) δ ppm: 3.55 (s, 3H, OCH_3), 3.87 (s, 6H, OCH_3), 6.50–7.26 (m, 3H, C=CH, and arom. CH), 7.69–8.12 (m, 4H, arom. CH), 9.18 (s, 1H, NH, D_2O exchangeable), 10.94 (s, 1H, NH, D_2O exchangeable), 12.10 (s, 1H, OH, D_2O exchangeable); ^{13}C NMR (DMSO-d_6) δ ppm: 56.47 (2 OCH_3), 60.39 (OCH_3), 104.88 (C2,6, benzene), 117.03 (C3,5, benzoic), 122.68 (C1, benzoic), 125.77 (C4, pyrazole), 128.66 (C1, benzene), 131.03 (C2,6, benzoic), 128.66 (C4, benzene), 142.10 (methylidene carbon), 145.30 (C4, benzoic), 147.93 (C3, pyrazole), 152.84 (C3,5, benzene), 163.56 (C=O, pyrazole), 167.61 (C=O, benzoic); anal. calcd. for $C_{20}H_{19}N_3O_6$ (379.13): C, 60.45; H, 4.78; N, 10.57; found C, 60.68; H, 4.89; N, 10.80.

*4-[(4Z)-4-(Benzylidene-5-oxo-1-phenyl-4,5-dihydro-1H-pyrazol-3-yl) amino]benzenesulfonamide (**3i**)*

Yield: 76%; red solid; m.p. 285–287°C; IR (KBr) cm^{-1}: 3,174, 3140, 3,113 (NH), 3,066–3,028 (arom. CH), 1,716 (C=O); ^{1}H NMR (DMSO-d_6) δ ppm: 7.20 (s, 1H, C=CH), 7.22–7.32 (m, 3H, arom. CH and SO_2NH_2, D_2O exchangeable), 7.46 (t, J = 7.4 Hz, 3H, arom. CH), 7.54–7.65 (m, 4H, arom. CH), 7.77 (t, J = 7.6 Hz, 3H, arom. CH), 7.89 (d, J = 16.8 Hz, 1H, arom. CH), 8.58 (d, J = 7.5 Hz, 2H, arom. CH), 11.61 (s, 1H, NH, D_2O exchangeable); ^{13}C NMR (DMSO-d_6) δ ppm: 118.82 (C3,5, benzenesulfonamide), 119.34 (C2,6, phenyl), 120.34 (C4, phenyl), 125.29 (C4, pyrazole), 129.16 (C2,6, benzene), 129.22 (C4, benzene), 129.30 (C2,6, benzenesulfonamide), 129.41 (C3,5, benzene), 133.87 (C1, benzenesulfonamide), 132.77 (C3,5, phenyl), 134.56 (C1, benzene), 137.09 (C1, phenyl), 137.43 (methylidene carbon), 149.56 (C4, benzenesulfonamide), 159.07 (C3, pyrazole), 160.87 (C=O, pyrazole); anal. calcd. for $C_{22}H_{18}N_4O_3S$ (418.11): C, 63.14; H, 4.34; N, 13.39; found C, 62.97; H, 4.50; N, 13.61.

*4-{[(4Z)-(2-Fluorobenzylidene)-5-oxo-1-phenyl-4,5-dihydro-1H-pyrazol-3-yl]amino}benzenesulfonamide (**3j**)*

Yield: 69%; brown solid; m.p. 199–201°C; IR (KBr) cm^{-1}: 3,367, 3,140, 3,113 (NH), 3,059–3,001 (arom. CH), 1,693 (C=O); ^{1}H NMR (DMSO-d_6) δ ppm: 7.23 (s, 1H, arom. CH), 7.47–7.54 (m, 4H, arom. CH and C=CH), 7.62–7.86 (m, 6H, arom. CH and SO_2NH_2, D_2O exchangeable), 7.92–7.99 (m, 4H, arom. CH), 8.51 (s, 1H, arom. CH), 11.85 (s, 1H, NH, D_2O exchangeable); ^{13}C NMR (DMSO-d_6) δ ppm: 118.09 (C3, benzene), 119.90 (C3,5, benzenesulfonamide), 122.00 (C2,6, phenyl), 122.06 (C1, benzene), 125.26 (C5, benzene), 125.47 (C4, phenyl), 128.18 (C4, pyrazole), 128.23 (C6, benzene), 129.33 (C2,6, benzenesulfonamide), 129.37 (C3,5, phenyl), 130.05 (C4, benzene), 134.23 (C1, benzenesulfonamide), 136.39 (C1, phenyl), 136.50 (methylidene carbon), 148.65 (C4, benzenesulfonamide), 151.84 (C3, pyrazole), 158.20 (C2, benzene), 164.47 (C=O, pyrazole); anal. calcd. for $C_{22}H_{17}FN_4O_3S$ (436.10): C, 60.54; H, 3.93; N, 12.84; found C, 60.68; H, 4.19; N, 13.06.

*4-{[(4Z)-(3-Fluorobenzylidene)-5-oxo-1-phenyl-4,5-dihydro-1H-pyrazol-3-yl]amino}benzenesulfonamide (**3k**)*

Yield: 66%; orange solid; m.p. 278–280°C; IR (KBr) cm^{-1}: 3,174, 3,140, 3,109 (NH), 3,070–3,032 (arom. CH), 1,716 (C=O); ^{1}H NMR (DMSO-d_6) δ ppm: 7.22 (t, J = 7.3 Hz, 2H, arom. CH), 7.44–7.50 (m, 5H, arom. CH, C=CH, and SO_2NH_2, D_2O exchangeable), 7.57–7.63 (m, 2H, arom. CH), 7.75 (t, J = 8.6 Hz, 3H, arom. CH), 7.89 (d, J = 18.3 Hz, 1H, arom. CH), 8.22 (d, J = 7.6 Hz, 1H, arom. CH), 8.60 (s, 1H, arom. CH), 8.69 (d, J = 10.7 Hz, 1H, arom. CH), 11.63 (s, 1H, NH, D_2O exchangeable); ^{13}C NMR (DMSO-d_6) δ ppm: 118.89 (C2, benzene), 119.71 (C4, benzene), 119.94 (C3,5, benzenesulfonamide), 120.48 (C2,6, phenyl), 120.69 (C6, benzene), 121.52 (C4, phenyl), 125.39 (C4, pyrazole), 129.34 (C2,6, benzenesulfonamide), 129.45 (C3,5, phenyl), 131.09 (C1, benzenesulfonamide), 131.17 (C5, benzene), 134.76 (C1, benzene), 134.85 (C1, phenyl), 137.28 (methylidene carbon), 158.85 (C4, benzenesulfonamide), 160.50 (C3, pyrazole), 160.99 (C3, benzene), 163.41 (C=O, pyrazole); anal. calcd. for $C_{22}H_{17}FN_4O_3S$ (436.1): C, 60.54; H, 3.93; N, 12.84; found C, 60.75; H, 4.12; N, 13.11.

*4-{[(4Z)-(2-Methoxybenzylidene)-5-oxo-1-phenyl-4,5-dihydro-1H-pyrazol-3-yl]amino}benzenesulfonamide (**3l**)*

Yield: 85%; brick red solid; m.p. 239–241°C; IR (KBr) cm^{-1}: 3,321, 3,136, 3,113 (NH), 3,032–3,001 (arom. CH), 2,877 (aliph. CH), 1,716 (C=O); ^{1}H NMR (DMSO-d_6) δ ppm: 3.94 (s, 3H, OCH_3), 7.05–7.1 (m, 2H, arom. CH), 7.15–7.22 (m, 3H, arom. CH), 7.42–7.47 (m, 3H, C=CH, and SO_2NH_2, D_2O exchangeable), 7.62 (t, J = 7.1 Hz, 2H, arom. CH), 7.74 (d, J = 7.8 Hz, 3H, arom. CH), 8.27 (d, J = 15.6 Hz, 1H, arom. CH), 8.94 (s, 1H, arom. CH), 8.09 (d, J = 7.8 Hz, 1H, arom. CH), 11.57 (s, 1H, NH, D_2O exchangeable); ^{13}C NMR (DMSO-d_6) δ ppm: 56.75 (OCH_3), 112.02 (C3, benzene), 118.72 (C1, benzene), 119.24 (C3,5, benzenesulfonamide), 120.75 (C5, benzene), 121.13 (C2,6, phenyl), 125.13 (C4, phenyl), 125.18 (C4, pyrazole), 129.29 (C2,6, benzenesulfonamide, C6, benzene), 129.40 (C4, benzene), 129.41 (C3,5, phenyl), 133.91 (C1, benzenesulfonamide), 136.60 (C1, phenyl), 142.83 (methylidene carbon), 143.32 (C4, benzenesulfonamide), 159.28 (C3, pyrazole), 160.46 (C2, benzene), 161.21 (C=O, pyrazole); anal. calcd. for $C_{23}H_{20}N_4O_4S$ (448.12): C, 61.59; H, 4.49; N, 12.49; found C, 61.68; H, 4.67; N, 12.69.

*4-{[(4Z)-(4-Methoxybenzylidene)-5-oxo-1-phenyl-4,5-dihydro-1H-pyrazol-3-yl]amino}benzenesulfonamide (**3m**)*

Yield: 71%; orange solid; m.p. 259–261°C; IR (KBr) cm^{-1}: 3,163, 3,120, 3,097 (NH), 3,078–3,024 (arom. CH), 2,866 (aliph. CH), 1,708 (C=O); ^{1}H NMR (DMSO-d_6) δ ppm: 3.89 (s, 3H, OCH_3), 7.11–7.15 (m, 3H, arom. CH and SO_2NH_2, D_2O exchangeable), 7.20 (t, J = 7.3 Hz, 2H, arom. CH), 7.43–7.48 (m, 3H, arom. CH and C=CH), 7.72–7.77 (m, 3H, arom. CH), 7.87 (d, J = 16.6 Hz, 2H, arom. CH), 8.64–8.70 (m, 3H, arom. CH), 11.26 (s, 1H, NH, D_2O exchangeable); ^{13}C NMR (DMSO-d_6) δ ppm: 56.23 (OCH_3), 115.01 (C3,5 benzene), 116.57 (C3,5, benzenesulfonamide), 118.74 (C2,6, phenyl), 119.26 (C4, phenyl), 125.09 (C4, pyrazole), 125.98 (C2,6, benzene), 126.02 (C1,

benzene), 129.30 (C2,6, benzenesulfonamide), 129.41 (C3,5, phenyl), 129.41 (C1, benzenesulfonamide), 137.70 (C1, phenyl), 137.79 (methylidene carbon), 159.77 (C4, benzenesulfonamide), 161.56 (C3, pyrazole), 164.34 (C4, benzene), 164.40 (C=O, pyrazole); anal. calcd. for $C_{23}H_{20}N_4O_4S$ (448.12): C, 61.59; H, 4.49; N, 12.49; found C, 61.80; H, 4.62; N, 12.71.

*4-{[(4Z)-(4-Chlorobenzylidene)-5-oxo-1-phenyl-4,5-dihydro-1H-pyrazol-3-yl]amino}benzenesulfonamide (**3n**)*

Yield: 70%; brick red solid; m.p. 280–282°C; IR (KBr) cm^{-1}: 3,379, 3,174, 3,128 (NH), 3,086–3,062 (arom. CH), 1,720 (C=O); ^1H NMR (DMSO-d_6) δ ppm: 7.22 (t, J = 7.3 Hz, 2H, arom. CH), 7.43–7.48 (m, 3H, arom. CH and SO_2NH_2, D_2O exchangeable), 7.62–7.65 (m, 3H, arom. CH, and C=CH), 7.73 (d, J = 7.9 Hz, 3H, arom. CH), 7.89 (d, J = 17.9 Hz, 2H, arom. CH), 8.61 (d, J = 8.6 Hz, 3H, arom. CH), 11.48 (s, 1H, NH, D_2O exchangeable); ^{13}C NMR (DMSO-d_6) δ ppm: 118.86 (C3,5, benzenesulfonamide), 120.72 (C2,6, phenyl), 125.34 (C4, phenyl), 125.51 (C4, pyrazole), 129.32 (C2,6, benzene), 129.34 (C2,6, benzenesulfonamide), 129.40 (C3,5, benzene), 129.46 (C3,5, phenyl), 131.67 (C1, benzenesulfonamide), 131.70 (C1, benzene), 136.13 (C4, benzene), 136.22 (C1, phenyl), 138.63 (methylidene carbon), 149.02 (C4, benzenesulfonamide), 149.41 (C3, pyrazole), 160.45 (C=O, pyrazole); anal. calcd. for $C_{22}H_{17}ClN_4O_3S$ (452.07): C, 58.34; H, 3.78; N, 12.37; found C, 58.61; H, 4.01; N, 12.56.

*4-{[(4Z)-(3,4-Dimethoxybenzylidene)-5-oxo-1-phenyl-4,5-dihydro-1H-pyrazol-3-yl]amino}benzenesulfonamide (**3o**)*

Yield: 78%; orange solid; m.p. 261–263°C; IR (KBr) cm^{-1}: 3,315, 3,163, 3,120 (NH), 3,093–3,016 (arom. CH), 2,866 (aliph. CH), 1,708 (C=O); ^1H NMR (DMSO-d_6) δ ppm: 3.86 (s, 3H, OCH_3), 3.90 (s, 3H, OCH_3), 7.14–7.17 (m, 2H, arom. CH), 7.21 (t, J = 7.3 Hz, 1H, arom. CH), 7.46 (t, J = 7.3 Hz, 3H, arom. CH, and C=CH), 7.72–7.78 (m, 4H, arom. CH and SO_2NH_2, D_2O exchangeable), 8.03–8.09 (m, 2H, arom. CH), 8.70 (s, 1H, arom. CH), 8.82 (d, J = 1.7 Hz, 2H, arom. CH), 11.27 (s, 1H, NH, D_2O exchangeable); ^{13}C NMR (DMSO-d_6) δ ppm: 55.98 (OCH_3), 56.37 (OCH_3), 111.97 (C2, benzene), 116.37 (C5, benzene), 116.75 (C3,5, benzenesulfonamide), 118.81 (C6, benzene), 119.48 (C2,6, phenyl), 125.10 (C4, phenyl), 126.16 (C4, pyrazole), 126.23 (C1, benzene), 129.32 (C2,6, benzenesulfonamide), 129.41 (C3,5, phenyl), 131.47 (C1, benzenesulfonamide), 131.71 (C1, phenyl, and methylidene carbon), 148.78 (C4, benzenesulfonamide), 148.81 (C4, benzene), 154.42 (C3, benzene), 159.94 (C3, pyrazole), 161.64 (C=O, pyrazole); anal. calcd. for $C_{24}H_{22}N_4O_5S$ (478.18): C, 60.24; H, 4.63; N, 11.71; found C, 60.09; H, 4.82; N, 11.89.

*4-{[(4Z)-(3,4,5-Trimethoxybenzylidene)-5-oxo-1-phenyl-4,5-dihydro-1H-pyrazol-3-yl]amino}benzenesulfonamide (**3p**)*

Yield: 74%; brown solid; m.p. 188–190°C; IR (KBr) cm^{-1}: 3,315, 3,163, 3,120 (NH), 3,066–3,001 (arom. CH), 2,939 (aliph. CH), 1,712 (C=O); ^1H NMR (DMSO-d_6) δ ppm: 3.81 (s, 3H, OCH_3), 3.86 (s, 6H, OCH_3), 7.22 (t, J = 7.4 Hz, 2H, arom. CH), 7.44–7.48 (m, 3H, arom. CH, and C=CH), 7.72–7.89 (m, 6H, arom. CH, and SO_2NH_2, D_2O exchangeable), 8.15–8.19 (d, J = 17.5 Hz, 3H, arom. CH), 11.44 (s, 1H, NH, D_2O exchangeable); ^{13}C NMR (DMSO-d_6) δ ppm: 56.51 (2 OCH_3), 60.79 (OCH_3), 112.85 (C2,6, benzene), 118.33 (C3,5, benzenesulfonamide), 118.90 (C2,6, phenyl), 119.58 (C4, phenyl), 125.22 (C4, pyrazole), 128.23 (C2,6, benzenesulfonamide), 128.31 (C3,5, phenyl), 129.33 (C1, benzene), 129.41 (C1, benzenesulfonamide), 137.14 (C1, phenyl), 137.53 (C4, benzene), 142.93 (methylidene carbon), 142.97 (C4, benzenesulfonamide), 152.91 (C3,5, benzene), 159.57 (C3, pyrazole), 161.23 (C=O, pyrazole); anal. calcd. for $C_{25}H_{24}N_4O_6S$ (508.14): C, 59.04; H, 4.76; N, 11.02; found C, 59.30; H, 4.89; N, 11.25.

4.2 | Biological evaluation

4.2.1 | In vitro COX-1 and COX-2 inhibitory assay

All the synthesized compounds were evaluated for their ability to inhibit COX-1 and COX-2 isoenzymes using 10-fold serial dilutions (1, 0.1, 0.01, 0.001 μg/ml) according to the manufacturer's instructions. Using the COX-1 (human) Inhibitor Screening Assay Kit and COX-2 (human) Inhibitor Screening Assay Kit (supplied by Cayman Chemical Company [catalog numbers 701070 and 701080, respectively], Ann Arbor, MI), the color was observed using Robonik P2000 ELISA reader. The method is based on measuring $PGF_{2\alpha}$ produced from stannous chloride reduction of COX-derived PGH2 produced in the COX reaction, which is based on the competition between PGs and a PG–acetylcholinesterase conjugate (PG tracer) for a limited amount of PG antiserum.

The compounds to be tested were dissolved in DMSO. The enzymes COX-1 and COX-2 (10 μl), heme (10 μl), and samples (20 μl) were incubated for 10 min at 37°C with the supplied reaction buffer solution (160 μl, 0.1 M Tris-HCl, pH 8 containing 5 mM ethylenediaminetetraacetic acid, and 2 mM phenol). Then, COX reactions were initiated by the addition of AA 100 μl, and the reaction was stopped after 30 s using stannous chloride. The $PGF_{2\alpha}$ formed in the samples by COX reactions was quantified by ELISA. After transfer to a 96-well plate, the plate was washed to remove any unbound reagent and then Ellman's reagent (200 μl), which contains substrate to acetyl cholinesterase, was added and incubated at room temperature for 60–90 min until the absorbance of the B_o well was in the range 0.3–0.8 A.U. at 410 nm. The plate was then read by an ELISA plate reader.[37,38]

The percentage inhibition was calculated for the different concentrations tested against control, and the IC_{50} against both COX-1 and COX-2 enzymes was calculated from the concentration inhibition curve.

4.2.2 | In vitro 5-LOX inhibitor screening assay

5-LOX inhibitor screening assay was performed to assess the inhibitory effect of synthesized compounds using a 5-Lipoxygenase Inhibitor Screening Kit (Fluorometric; BioVision, CA) according to the manufacturer's procedures (catalog number K980-100). The assay

depends on the recording fluorescence every 30 s and then ΔRFU for all the compounds used using Topotecan, Spark 10M, a multimode microplate reader.[39]

4.2.3 | In vivo AI assay

The animal treatment protocol was approved by the Faculty of Pharmacy, Cairo University, Animal Rights committee (OC2085). In all tests, adequate considerations were adopted to reduce pain or discomfort of animals. All quantitative results obtained from the biological evaluation were calculated as the mean ± standard error. The statistical significance between the data for celecoxib and test compounds was assessed by one-way analysis of variance ($p < 0.05$).

Adult male albino rats of Sprague Dawley strain weighing 130–150 g[40,41] were kept in the animal house unit of the pharmacology and toxicology department for a least 1 week before the experiments under standard conditions of light and temperature. All animals were accessed to standard laboratory diet consisting of vitamin mixture (1%), mineral mixture (4%), corn oil (10%), sucrose (20%), cellulose (0.2%), casein 95% pure (10.5%), and starch (54.3%). All test compounds were suspended in 10% Tween-80 solution in distilled water. Compounds **3f**, **3h**, **3l**, and **3p** were evaluated for their in vivo AI activity by applying the carrageenan-induced rat paw edema screening protocol as an acute inflammation model[42] according to a previously reported method after oral administration of a dose of 10 mg/kg of tested compounds as well as reference drugs.[40,43,44] The rats were marked and divided into eight experimental groups of six rats each. The first group received 1 ml saline and served as untreated control. The second to sixth groups received 10 mg/kg of tested compounds **3f**, **3h**, **3l**, and **3p**, respectively. The last two groups received 10 mg/kg of the reference drugs celecoxib and indomethacin, respectively, and served as reference standard groups. After 1 hr of oral administration of all previous compounds, a subplantar injection of 0.1 ml of 1% carrageenan solution to the right hind paw of each animal was done. The paw volume was recorded using a plethysmometer (UGO Basile 7140) at 0, 1, 2, 3, and 4 hr and the percentage edema inhibition was calculated using the following equation: AI activity (%) = $(1 - D_t/D_c)/100$, where D_t represents the difference in paw volume before and after drug was administered to the rats and D_c represents the difference of volume in the control groups.

4.2.4 | Gastric ulcerogenic activity

Compounds **3f**, **3h**, **3l**, and **3p** were also evaluated for the development of acute gastric ulcer upon oral administration in adult male albino rats. Rats were starved for 18 hr prior and were divided into eight groups of seven rats each and tested compounds, references (celecoxib and indomethacin) or saline as control were administered orally at a dose of 10 mg/kg body weight. Four hours after the treatment, the animals were killed and their stomachs were removed and examined macroscopically using a magnifying lens. A longitudinal incision along the greater curvature was made with a fine scissor. The presence of a single or multiple lesions, erosion, ulcer, or perforation was evaluated.[45] The number of ulcers and the occurrence of hyperemia were noted. The gastric lesions were stretched out and scored from 0 (*no lesion*) to 5 (*3 or more marked ulcers*), according to the method of Clementi et al.[46]

4.2.5 | Determination of rat serum PGE2

Rat serum levels of PGE2 were determined using blood samples collected from the rats subjected to carrageenan rat paw edema model 4 hr after carrageenan injection using a PGE2-specific enzyme immunoassay kit according to the manufacturer's protocol (catalog number 514095; Cayman Chemical). The optical density was determined after 1 hr using a microplate reader DYNATech, MR 5000 (Dynatech Industries Inc., McLean, VA) at 450 nm, and expressed as pg/ml.

4.3 | Molecular docking study into COX-2 and 5-LOX active sites

The docking experiment of the compounds showing the highest selectivity ratio toward COX-2 enzymes (**3f**, **3h**, **3l**, and **3p**), as well as SC-558, and celecoxib, was performed using MOE (10.2008) software (Chemical Computing Group, Montreal, Canada) using the crystal structure of COX-2 enzyme (PDB entry 1CX2)[31] and the crystal structure of 5-LOX enzyme (PDB entry 3V99)[47] downloaded from the Protein Data Bank (PDB) website (https://www.rcsb.org/). The protein structure was prepared by deleting the repeating chains and water molecules. The database of active compounds was prepared by adding hydrogen using Protonate 3D application. Calculating the partial charges and minimizing energy by Merck molecular force field (MMFF94X) until RMSD gradient of 0.05 $kcal \cdot mol^{-1} \cdot Å^{-1}$ followed by isolation of the determined pocket and the backbone was hidden. Ligands were docked within this active site using MOE-Dock option under default setting, utilizing triangle matcher as the method of displacement and London dG as the main scoring function. The resulting database contained the scores between the ligand conformers and the enzyme binding site in kcal/mol. Many conformers of each compound were obtained and the best ligand–enzyme interaction was the best score and was set as default.

ACKNOWLEDGMENTS

The authors are grateful to Dr. Essam Rashwan, head of the confirmatory diagnostic unit Vacsera-Egypt, for carrying out the in vitro COX-1 and COX-2 inhibitory assay. The authors would like to thank Dr. Amr Sayed Motawi, lecturer of Pharmaceutical Organic Chemistry, Department of Pharmaceutical Organic Chemistry, Faculty

of Pharmacy, Cairo University for helping in the molecular docking study.

CONFLICT OF INTERESTS

The authors declare that there are no conflict of interests.

ORCID

Khaled O. Mohamed http://orcid.org/0000-0002-2293-5363

REFERENCES

[1] C. Pereira-Leite, C. Nunes, S. K. Jamal, I. M. Cuccovia, S. Reis, *Med. Res. Rev.* **2017**, *37*, 802.
[2] A. Whelton, A. J. Watson, *Clinical Nephrotoxins*, Springer, Dordrecht, The Netherlands **1998**, pp. 203–216.
[3] E. A. Meade, W. L. Smith, D. L. Dewitt, *J. Biol. Chem.* **1993**, *268*, 6610.
[4] R. S. Bresalier, R. S. Sandler, H. Quan, J. A. Bolognese, B. Oxenius, K. Horgan, C. Lines, R. Riddell, D. Morton, A. Lanas, M. A. Konstam, J. A. Baron, *N. Engl. J. Med.* **2005**, *352*, 1092.
[5] J.-M. Dogné, C. T. Supuran, D. Pratico, *J. Med. Chem.* **2005**, *48*, 2251.
[6] S. Harirforoosh, W. Asghar, F. Jamali, *J. Pharm. Pharm. Sci.* **2014**, *16*, 821.
[7] G. De Gaetano, M. B. Donati, C. Cerletti, *Trends Pharmacol. Sci.* **2003**, *24*, 245.
[8] J. Martel-Pelletier, D. Lajeunesse, P. Reboul, J.-P. Pelletier, *Ann. Rheum. Dis.* **2003**, *62*, 501.
[9] K. Yang, W. Ma, H. Liang, Q. Ouyang, C. Tang, L. Lai, *PLOS Comput. Biol.* **2007**, *3*, e55.
[10] S. Laufer, S. Gay, K. Brune, *Inflammation and Rheumatic Diseases: The Molecular Basis of Novel Therapies*, Georg Thieme Verlag, Stuttgart, NY **2003**.
[11] F. Celotti, S. Laufer, *Pharmacol. Res.* **2001**, *43*, 429.
[12] A. Blackham, R. J. Griffiths, C. Hallam, J. Mann, P. D. Mitchell, A. A. Norris, W. T. Simpson, *Agents Actions* **1990**, *30*, 432.
[13] D. C. Argentieri, D. M. Ritchie, M. P. Ferro, T. Kirchner, M. P. Wachter, D. W. Anderson, M. E. Rosenthale, R. J. Capetola, *J. Pharmacol. Exp. Ther.* **1994**, *271*, 1399.
[14] J. L. Wallace, D.-M. McCafferty, L. Carter, W. McKnight, D. Argentieri, *Gastroenterology* **1993**, *105*, 1630.
[15] D. W. Anderson, D. C. Argentien, D. M. Ritchie, L. B. Katz, D. A. Shriver, M. E. Rosenthale, R. J. Capetola, *FASEB J.* **1990**, *4*, A1122.
[16] A. Araico, M. C. Terencio, M. J. Alcaraz, J. N. Dominguez, C. Leon, M. L. Ferrandiz, *Life Sci.* **2006**, *78*, 2911.
[17] A. Araico, M. C. Terencio, M. J. Alcaraz, J. N. Dominguez, C. León, M. L. Ferrándiz, *Life Sci.* **2007**, *80*, 2108.
[18] M. A. Shaaban, L. N. Soliman, S. M. A. Roshdy, K. O. A. Mohamed, *Bull. Fac. Pharm.* **2009**, *47*, 35.
[19] P. Gupta, J. K. Gupta, A. K. Halve, *Int. J. Pharm. Sci.* **2015**, *6*, 2291.
[20] E. Arbačiauskienė, S. Krikštolaitytė, A. Mitrulevičienė, A. Bieliauskas, V. Martynaitis, M. Bechmann, A. Roller, A. Šačkus, W. Holzer, *Molecules* **2018**, *23*, 129.
[21] G. Mariappan, B. P. Saha, L. Sutharson, A. Haldar, 2010, 49B, 1671.
[22] A. Mandour, E. El-Sawy, M. Ebaid, S. Hassan, *Acta Pharm.* **2012**, *62*, 15.
[23] T. Srivalli, K. Satish, R. Suthakaran, *Int. J. Innov. Pharm. Res.* **2011**, *2*, 172.
[24] S. K. Sahu, M. Banerjee, A. Samantray, C. Behera, M. A. Azam, *Trop. J. Pharm. Res.* **2008**, *7*, 961.
[25] C. Charlier, C. Michaux, *Eur. J. Med. Chem.* **2003**, *38*, 645.
[26] M. A. Abdelgawad, M. B. Labib, W. A. M. Ali, G. Kamel, A. A. Azouz, E.-N. EL-Shaymaa, *Bioorg. Chem.* **2018**, *78*, 103.
[27] H. Chen, Q. Li, X. Yao, B. Fan, S. Yuan, A. Panaye, J. P. Doucet, *QSAR Comb. Sci.* **2004**, *23*, 36.
[28] O. Llorens, J. J. Perez, A. Palomer, D. Mauleon, *Bioorg. Med. Chem. Lett.* **1999**, *9*, 2779.
[29] R. G. Kurumbail, A. M. Stevens, J. K. Gierse, J. J. McDonald, R. A. Stegeman, J. Y. Pak, D. Gildehaus, T. D. Penning, K. Seibert, P. C. Isakson, *Nature* **1996**, *384*, 644.
[30] R. M. Garavito, D. L. DeWitt, *Biochim. Biophys. Acta, Mol. Cell Biol. Lipids* **1999**, *1441*, 278.
[31] G. Moussa, R. Alaaeddine, L. M. Alaeddine, R. Nassra, A. S. F. Belal, A. Ismail, A. F. El-Yazbi, Y. S. Abdel-Ghany, A. Hazzaa, *Eur. J. Med. Chem.* **2018**, *144*, 635.
[32] S. W. Rowlinson, J. R. Kiefer, J. J. Prusakiewicz, J. L. Pawlitz, K. R. Kozak, A. S. Kalgutkar, W. C. Stallings, R. G. Kurumbail, L. J. Marnett, *J. Biol. Chem.* **2003**, *278*, 45763.
[33] R. Soliva, C. Almansa, S. G. Kalko, F. J. Luque, M. Orozco, *J. Med. Chem.* **2003**, *46*, 1372.
[34] T. Shimokawa, R. J. Kulmacz, D. L. Dewitt, W. L. Smith, *J. Biol. Chem.* **1990**, *265*, 20073.
[35] S. B. Ganorkar, Y. Vander Heyden, A. A. Shirkhedkar, D. K. Lokwani, D. M. Dhumal, P. S. Bobade, *J. Pharm. Biomed. Anal.* **2019**, 112982.
[36] M. K. S. El-Nagar, H. H. M. Abdu-Allah, O. I. A. Salem, A.-H. N. Kafafy, H. S. M. Farghaly, *Bioorg. Chem.* **2018**, *78*, 80.
[37] A.-M. Alaa, L. A. Abou-Zeid, K. E. H. ElTahir, R. R. Ayyad, A.-A. Magda, A. S. El-Azab, *Eur. J. Med. Chem.* **2016**, *121*, 410.
[38] M. H. Abdelrahman, B. G. M. Youssif, A. H. Abdelazeem, H. M. Ibrahim, A. M. Abd El Ghany, L. Treamblu, S. N. A. Bukhari, *Eur. J. Med. Chem.* **2017**, *127*, 972.
[39] B. Roschek Jr, R. C. Fink, D. Li, M. McMichael, C. M. Tower, R. D. Smith, R. S. Alberte, *J. Med. Food* **2009**, *12*, 615.
[40] M. Koksal, I. Ozkan-Dagliyan, T. Ozyazici, B. Kadioglu, H. Sipahi, A. Bozkurt, S. S. Bilge, *Arch. Pharm. Chem. Life Sci.* **2017**, *350*, e1700153.
[41] E. M. Ahmed, A. E. Kassab, A. A. El-Malah, M. S. A. Hassan, *Eur. J. Med. Chem.* **2019**, *171*, 25.
[42] C. A. Winter, E. A. Risley, G. W. Nuss, *Proc. Soc. Exp. Biol. Med.* **1962**, *111*, 544.
[43] L. W. Mohamed, M. A. Shaaban, A. F. Zaher, S. M. Alhamaky, A. M. Elsahar, *Bioorg. Chem.* **2019**, *83*, 47.
[44] T. H. Ibrahim, Y. M. Loksha, H. A. Elshihawy, D. M. Khodeer, M. M. Said, *Arch. Pharm. Chem. Life Sci.* **2017**, *350*, e1700093.
[45] E. Manivannan, S. C. Chaturvedi, *Bioorg. Med. Chem.* **2011**, *19*, 4520.
[46] G. Clementi, A. Caruso, V. M. C. Cutuli, E. de Bernardis, A. Prato, N. G. Mangano, M. Amico-Roxas, *Eur. J. Pharmacol.* **1998**, *360*, 51.
[47] H. A. Abd El Razik, M. H. Badr, A. H. Atta, S. M. Mouneir, M. M. Abu-Serie, *Arch. Pharm. Chem. Life Sci.* **2017**, *350*, e1700026.

SUPPORTING INFORMATION

Additional supporting information may be found online in the Supporting Information section.

How to cite this article: Shabaan MA, Kamal AM, Faggal SI, Elsahar AE, Mohamed KO. Synthesis and biological evaluation of pyrazolone analogues as potential anti-inflammatory agents targeting cyclooxygenases and 5-lipoxygenase. *Arch Pharm Chem Life Sci*. 2020;353:e1900308. https://doi.org/10.1002/ardp.201900308